

Supporting Information (SI)

**Hydrodeoxygenation of Phenol over Ni-Based Bimetallic Single-Atom
Surface Alloys: Mechanism, Kinetics and Descriptor**

Jingwen Zhou, Wei An, Zeming Wang, Xin Jia*

College of Chemistry and Chemical Engineering, Shanghai University of Engineering Science,
Songjiang District, Shanghai 201620, China

*E-mail: weian@sues.edu.cn

Table S1. DFT-calculated surface segregation energy, OH-induced segregation energy, magnetic moment and Bader charge transfer of M@Ni(111) surface alloy.

M@Ni(111)	Fe	V	Mo	W	Re
E_{Segr} (eV)	0.24	0.65	0.68	0.83	0.74
OH- E_{Segr} (eV) ^a	-0.47	-1.43	-0.82	-0.61	0.14
$\Delta\mu$ (μ_B) ^b	-0.81	-1.44	-1.60	-1.42	-1.96
Δq (e ⁻) ^c	-0.35	-0.95	-0.61	-0.60	-0.14

^a with full coverage of OH*.

^b $\Delta\mu$: decrease in magnetic moment due to adsorption of phenol.

^c Δq : negative number denotes charge transferred from doped metals (per atom) to host Ni.

Table S2. DFT-calculated binding energy (BE) for surface species of H*, OH*, O*, H₂O*, C₆H₅OH*, and C₆H₆* adsorbed on M@Ni(111) and Ni(111), where M = Fe, V, Mo, W, Re.

BE(eV)	M@Ni(111)					Ni(111)
	Fe	V	Mo	W	Re	
H ^a	-0.53	-0.63	-0.64	-0.62	-0.63	-0.56
OH ^b	-3.51	-4.01	-3.81	-4.15	-3.53	-3.37
O ^c	-5.43	-6.36	-6.21	-6.49	-6.03	-5.28
H ₂ O	-0.43	-0.78	-0.77	-0.79	-0.61	-0.31
1 phenol ^d	-0.98	-1.32	-1.25	-1.22	-1.07	-0.92
	<i>-1.86</i>	<i>-2.20</i>	<i>-2.13</i>	<i>-2.08</i>	<i>-1.94</i>	<i>-1.79</i>
6 benzene ^d	-1.05	-1.16	-1.12	-1.09	-1.07	-1.04
	<i>-1.83</i>	<i>-1.93</i>	<i>-1.89</i>	<i>-1.85</i>	<i>-1.84</i>	<i>-1.82</i>

^a BE(H) = E(H/slab) - E(slab) - 0.5E(H₂).

^b BE(OH) = E(OH/slab) - E(slab) - [E(OH)].

^c BE(O) = E(O/slab) - E(slab) - [E(O)].

^d Italic number: calculated using optB88-vdW functional; Plain number: calculated using GGA-PBE functional.

Table S3. DFT-calculated binding energy (BE) for stable products adsorbed on Ni(111) and Mo@Ni(111), as in Table S2

BE(eV)	cyclohexanone	cyclohexane	benzene	cyclohexanol
Ni(111)	-0.96	-0.77	-1.83	-1.10
	-0.26	-0.09	-1.05	-0.27
Mo@Ni(111)	-1.55	-0.80	-1.89	-1.53
	-0.94	-0.12	-1.12	-0.82

Table S4. Binding energy (BE), zero-point energy (Δ ZPE), entropy corrections (T Δ S), for desorption free energy barrier (G) calculation at T = 573 K.

Mo@Ni(111)	BE(eV)	Δ ZPE(eV)	T Δ S(eV)	G(eV)
cyclohexanone	-1.55	-0.03	0.38	1.14
cyclohexane	-0.80	0.07	0.36	0.51
benzene	-1.89	0.01	0.37	1.53
cyclohexanol	-1.53	-0.04	0.48	1.01

Table S5. DFT-calculated reaction energy (E_{rxn}) for direct deoxygenation (DDO), partial hydrodeoxygenation (PHDO), H₂O formation and OH* binding energy (BE) on Ni(111) and M@Ni(111), where M is 3d transition metals.

M@Ni(111)	E_{rxn} (DDO)	E_{rxn} (PHDO)	E_{rxn} (H ₂ O)	BE(OH*)
	eV			
Sc	0.01	-1.01	0.57	-4.11
Ti	-0.09	-0.97	0.63	-4.14
V	-0.10	-0.89	0.62	-4.01
Cr	0.02	-0.77	0.46	-3.82
Mn	0.28	-0.82	0.38	-3.59
Fe	0.53	-0.79	0.37	-3.51
Co	0.60	-0.75	0.35	-3.42
Ni	0.61	-0.75	0.36	-3.37

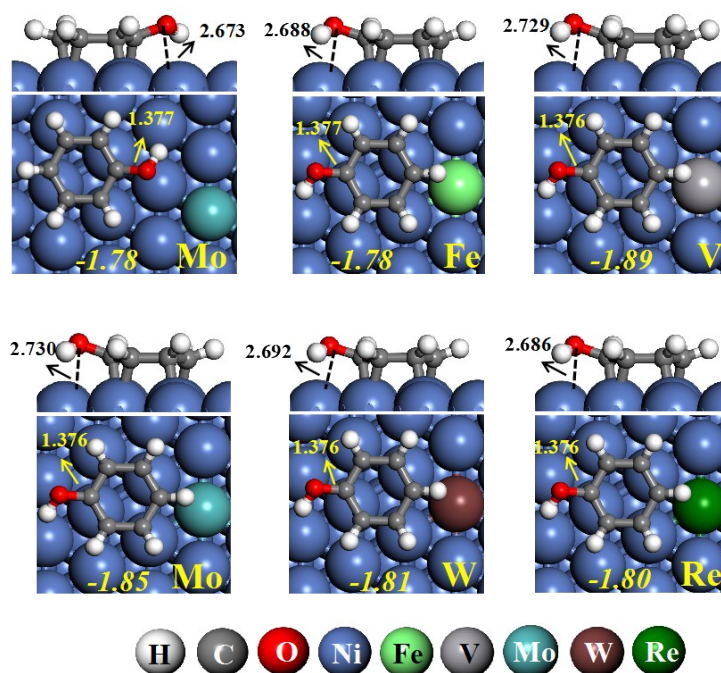


Figure S1. Optimized configurations of phenol adsorption on $M@Ni(111)$ with hydroxyl O interacting with Ni atoms. Regular numeric: C-OH bond length and M-O binding distance (in Å); Italic numeric: binding energy (in eV) calculated using optB88-vdW functional.

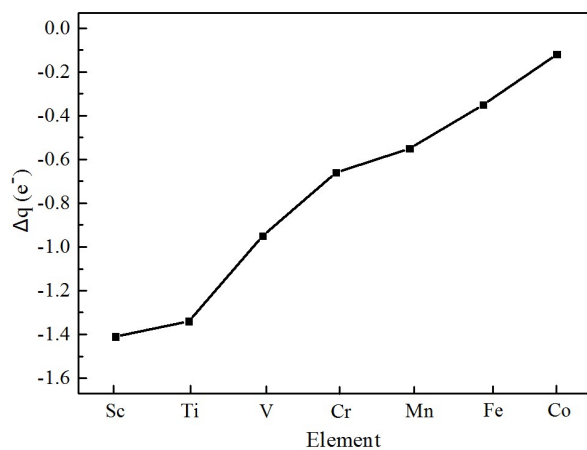
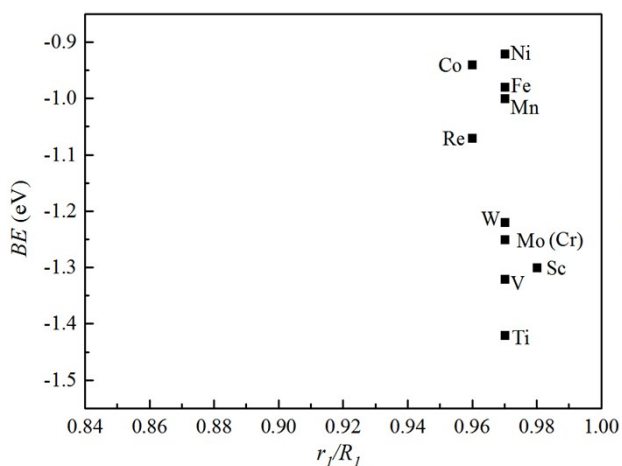
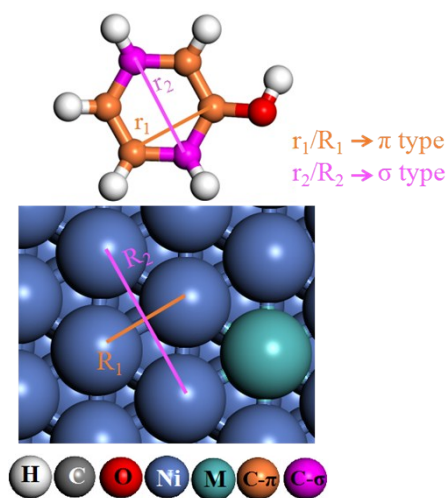
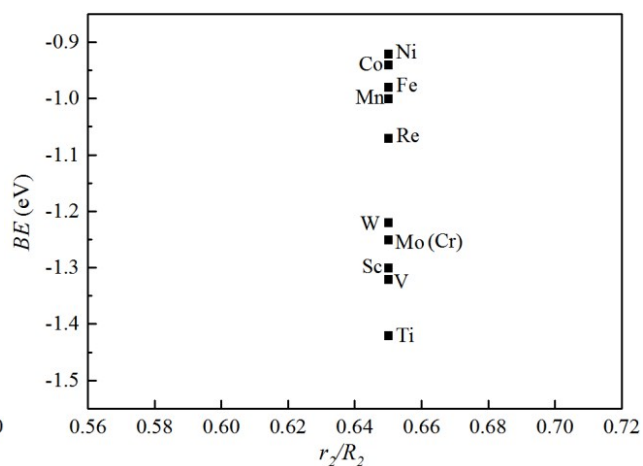


Figure S2. Variation of electron charges (Δq , per M atom) transferred from $3d$ metals (M) to host Ni of $M@Ni(111)$ single-atom surface alloy, indicative of stronger oxophilicity of M elements studied than Ni host.

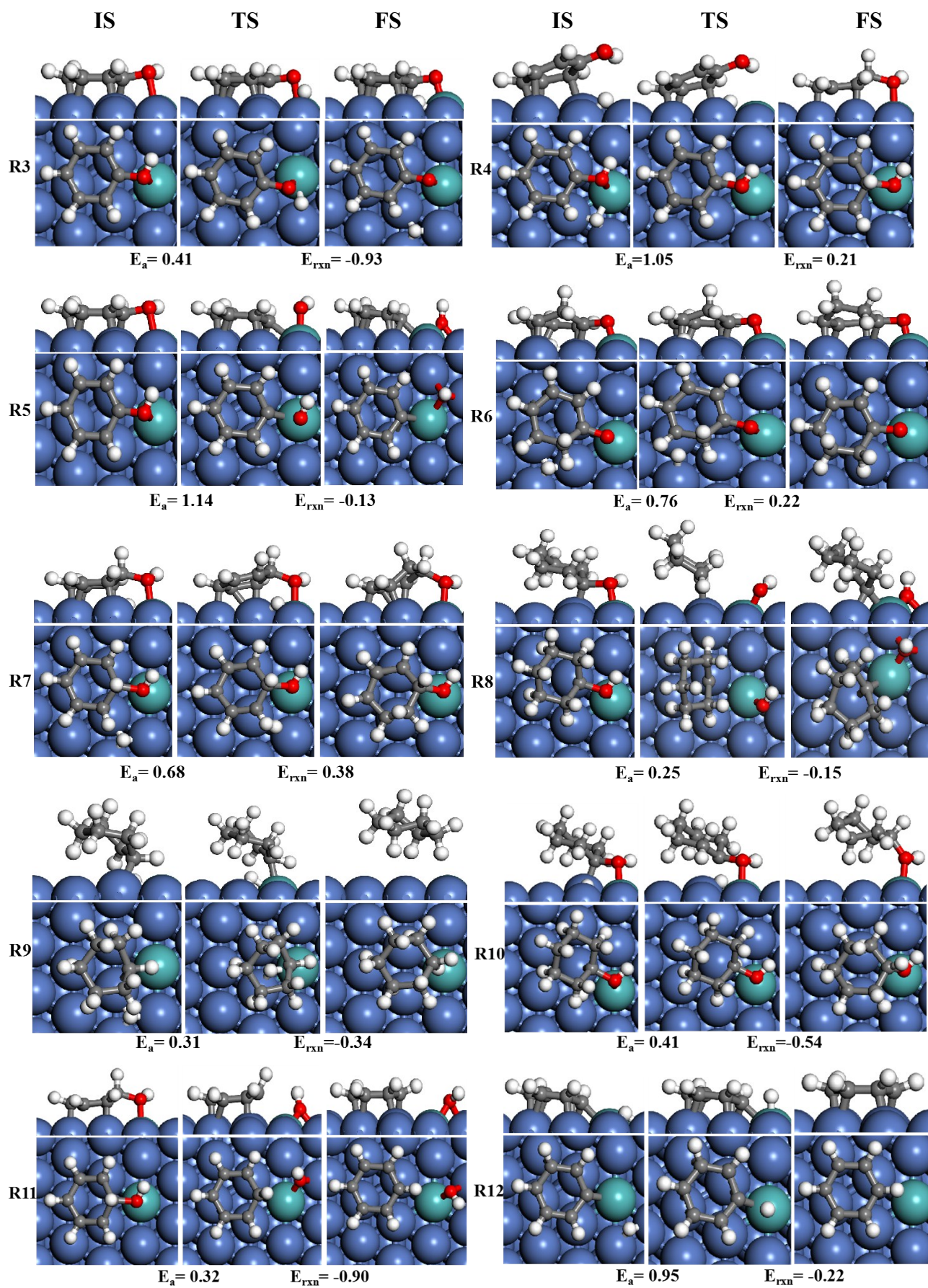


(b)



(c)

Figure S3. (a) Schematics of geometric match between phenyl ring (r_1 and r_2) and rhombus-shaped adsorption site (R_1 and R_2) at bri30 adsorption configuration, where r_1/R_1 and r_2/R_2 have impact on C-M-C bidentate π -type binding and C-M monodentate σ -type binding, respectively; (b) and (c) Variation of binding energy (BE) of phenol with geometric match between phenyl ring (r_1 and r_2) and rhombus-shaped adsorption site (R_1 and R_2) at bri30 adsorption configuration.



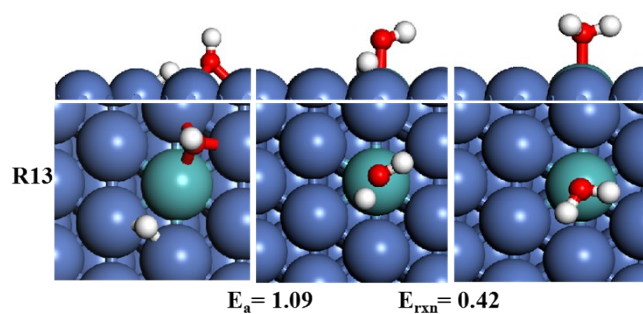


Figure S4. DFT-optimized structures for initial state (IS), transition state (TS), and final state (FS) on the Mo@Ni(111). The activation barrier (E_a , in eV) and reaction energy (E_{rxn} , in eV) without ZPE-correction are displayed.

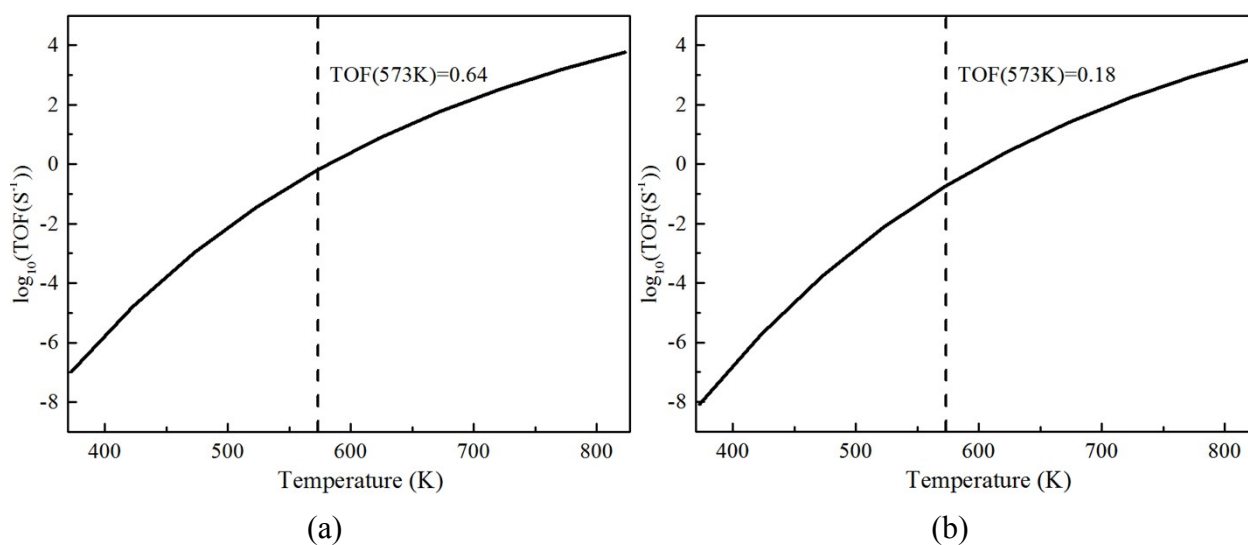


Figure S5. Variation of turnover frequency (TOF) with temperature for phenol HDO on Mo@Ni(111) to form (a) total products of cyclohexane, cyclohexanol and benzene; (b) benzene. Dashed line: 573K. Reaction conditions: 1/9 atm phenol and 1 atm H_2 .

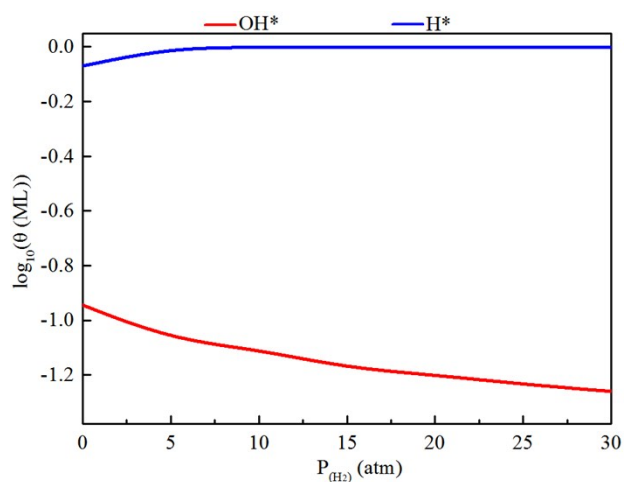


Figure S6. Logarithm of OH* and H* coverage (θ) as a dependence of H_2 pressure over Mo@Ni(111). Reaction conditions: 1/9 atm phenol, $T = 573$ K.

S1. Microkinetic analysis

Based on the transition state theory and statistical mechanics formalism, we performed a microkinetic analysis using the DFT-calculated energetics of elementary steps in a simplified reaction network (Scheme 1). In the network, we proposed several key surface species, i.e., H*, OH*, **1***, **2***, **5***, **8***, **9***, **10***, that are important in determining the product distribution observed in experiment. The site balance of intermediate species included in the reaction mechanism can be estimated in terms of coverage (θ_X ; **X** = surface species), which has been applied to the similar microkinetic modeling.¹⁻⁵ Two different sites have been considered: (i) sites for all aromatic adsorbates (and free sites on Ni(111) and M@Ni(111) surfaces), and (ii) sites for H* adsorption. In this approach, H* is adsorbed on a special “hydrogen reservoir” site, not competing with other adsorbates for free sites. The major products, i.e., cyclohexanol (OL) (**11**), cyclohexane (ANE) (**12**), benzene (BZ) (**13**), H₂O will desorb from the active sites upon formed releasing the free sites.

The adsorption of phenol (**R1**) and the dissociative adsorption of H₂ (**R2**) are assumed to follow Langmuir adsorption mode and in thermodynamics equilibriums. As such, we can estimate the adsorption constant based on the calculated adsorption energies and the estimated entropy changes from gas phase to the adsorbed species by approximating the change as condensation. Thus, the equilibrium constant was estimated based on $K = \exp[-(\Delta E_{ads} - T\Delta S)/k_B T]$, where ΔE_{ads} is ZPE-corrected adsorption energy of phenol or ZPE-corrected reaction energy of H₂ dissociation on M@Ni(111), and ΔS is the entropy change of adsorbed and gas-phase phenol or H₂. The entropy change for gas-phase H₂, phenol and major products are obtained or calculated from NIST Chemistry WebBook:⁶

$$\Delta S(0 \rightarrow T, P^0) = \Delta S_{ads}(0 \rightarrow T, P^0) - \Delta S_{gas}(0 \rightarrow T, P^0) \quad (1)$$

The entropy change for adsorbed gas-phase was calculated according to:

$$\Delta S_{ads}(0 \rightarrow T, P^0) = S_{vib} = \sum_{i=1}^{3N} \left[\frac{N_A h \nu_i}{T(e^{h\nu_i/k_B T} - 1)} - R \ln(1 - e^{-h\nu_i/k_B T}) \right] \quad (2)$$

where ν_i is the normal-mode frequency for species of 3N degree of freedom (N=number of atoms) adsorbed on Ni(111) or Mo@Ni(111).

The zero-point energy (ZPE) corrections were included in the calculations of activation and reaction energies. The reaction rate constant k_n and pre-exponential factor A can be estimated from the normal-mode frequencies, ν_i , at the initial (IS) and transition (TS) states according to the following equation:

$$k_n = \frac{k_B T}{h} \frac{Q_{TS}}{Q_{IS}} \exp(-E_{a,n}^0 / k_B T) = A \exp(-E_{a,n}^0 / k_B T) \quad (3)$$

$$A = \frac{k_B T}{h} \frac{Q_{TS}}{Q_{IS}} \quad (4)$$

where $E_{a,n}^0$, T, k_B , h denotes the zero-point energy (ZPE) corrected activation barrier, reaction temperature, Boltzmann constant, and Planck's constant, respectively. The vibrational partition functions of the transition and initial states, Q_{TS} and Q_{IS} , can be evaluated using the calculated harmonic frequencies based on:

$$Q_{vib} = \prod_i \frac{1}{1 - e^{-h\nu_i/k_B T}} \quad (5)$$

where i runs to $3N-1$ and $3N$ for the transition state and initial state, respectively, N is the number of atoms for adsorbates.

Based on the steady state approximation and microscopic reversibility, we can establish the following equations for the elementary reaction steps (**R1 – R13**):

$$r_1 = k_1^+ P_1 \theta_* - k_1^- \theta_1 \quad (6)$$

$$r_2 = k_2^+ P_{H_2} \theta_{*h}^2 - k_2^- \theta_H^2 \quad (7)$$

$$r_3 = k_3^+ \theta_1 \theta_{*h} - k_3^- \theta_5 \theta_{*h} \quad (8)$$

$$r_4 = k_4^+ \theta_1 \theta_H - k_4^- \theta_2 \theta_{*h} \quad (9)$$

$$r_5 = k_5^+ \theta_1 \theta_{*h} - k_5^- \theta_{10} \theta_{OH} \quad (10)$$

$$r_6 = k_6^+ \theta_5 \theta_H - k_6^- \theta_8 \theta_{*h} \quad (11)$$

$$r_7 = k_7^+ \theta_2 \theta_H - k_7^- \theta_* \theta_{*h} \quad (12)$$

$$r_8 = k_8^+ \theta_8 \theta_{*h} - k_8^- \theta_9 \theta_{OH} \quad (13)$$

$$r_9 = k_9^+ \theta_9 \theta_H - k_9^- \theta_* \theta_{*h} \quad (14)$$

$$r_{10} = k_{10}^+ \theta_8 \theta_H - k_{10}^- \theta_* \theta_{*h} \quad (15)$$

$$r_{11} = k_{11}^+ \theta_2 \theta_{*h} - k_{11}^- \theta_* \theta_{OH} \quad (16)$$

$$r_{12} = k_{12}^+ \theta_{10} \theta_H - k_{12}^- \theta_* \theta_{*h} \quad (17)$$

$$r_{13} = k_{13}^+ \theta_{OH} \theta_H - k_{13}^- \theta_* \theta_{*h} \quad (18)$$

By applying the pseudo-steady state approximation:

$$\frac{d\theta_2}{dt} = r_4 - r_7 - r_{11} = 0$$

$$\Rightarrow k_4^+ \theta_1 \theta_H - k_4^- \theta_2 \theta_{*h} - k_7^+ \theta_2 \theta_H + k_7^- \theta_* \theta_{*h} - k_{11}^+ \theta_2 \theta_{*h} + k_{11}^- \theta_* \theta_{OH} = 0$$

$$\frac{d\theta_5}{dt} = r_3 - r_6 = 0$$

$$\Rightarrow k_3^+ \theta_1 \theta_{*h} - k_3^- \theta_5 \theta_{*h} - k_6^+ \theta_5 \theta_H + k_6^- \theta_8 \theta_{*h} = 0$$

$$\frac{d\theta_8}{dt} = r_6 - r_8 - r_{10} = 0$$

$$\Rightarrow k_6^+ \theta_5 \theta_H - k_6^- \theta_8 \theta_{*h} - k_8^+ \theta_8 \theta_{*h} + k_8^- \theta_9 \theta_{OH} - k_{10}^+ \theta_8 \theta_H + k_{10}^- \theta_* \theta_{*h} = 0$$

$$\frac{d\theta_9}{dt} = r_8 - r_9 = 0$$

$$\Rightarrow k_8^+ \theta_8 \theta_{*h} - k_8^- \theta_9 \theta_{OH} - k_9^+ \theta_9 \theta_H + k_9^- \theta_* \theta_{*h} = 0$$

$$\frac{d\theta_{10}}{dt} = r_5 - r_{12} = 0$$

$$\Rightarrow k_5^+ \theta_1 \theta_{*h} - k_5^- \theta_{10} \theta_{OH} - k_{12}^+ \theta_{10} \theta_H + k_{12}^- \theta_* \theta_{*h} = 0$$

$$\frac{d\theta_{OH}}{dt} = r_5 + r_{11} + r_8 - r_{13} = 0$$

$$\Rightarrow k_5^+ \theta_1 \theta_{*h} - k_5^- \theta_{10} \theta_{OH} + k_8^+ \theta_8 \theta_{*h} - k_8^- \theta_9 \theta_{OH} + k_{11}^+ \theta_2 \theta_{*h} - k_{11}^- \theta_* \theta_{OH} - k_{13}^+ \theta_H \theta_{OH} + k_{13}^- \theta_* \theta_{*h} = 0$$

We obtain:

$$\begin{aligned} \Rightarrow \theta_2 &= \frac{k_4^+ \theta_1 \theta_H + k_7^- \theta_* \theta_{*h} + k_{11}^- \theta_* \theta_{OH}}{k_4^- \theta_{*h} + k_7^+ \theta_H + k_{11}^+ \theta_{*h}} \\ \Rightarrow \theta_5 &= \frac{k_3^+ \theta_1 \theta_{*h} + k_6^- \theta_8 \theta_{*h}}{k_3^- \theta_{*h} + k_6^+ \theta_H} \\ \Rightarrow \theta_8 &= \frac{k_6^+ \theta_5 \theta_H + k_8^- \theta_9 \theta_{OH} + k_{10}^- \theta_* \theta_{*h}}{k_6^- \theta_{*h} + k_8^+ \theta_{*h} + k_{10}^+ \theta_H} \\ \Rightarrow \theta_9 &= \frac{k_8^+ \theta_8 \theta_{*h} + k_9^- \theta_* \theta_{*h}}{k_8^- \theta_{OH} + k_9^+ \theta_H} \\ \Rightarrow \theta_{10} &= \frac{k_5^+ \theta_1 \theta_{*h} + k_{12}^- \theta_* \theta_{*h}}{k_5^- \theta_{OH} + k_{12}^+ \theta_H} \\ \Rightarrow \theta_{OH} &= \frac{k_5^+ \theta_1 \theta_{*h} + k_8^+ \theta_8 \theta_{*h} + k_{11}^+ \theta_2 \theta_{*h} + k_{13}^- \theta_* \theta_{*h}}{k_5^- \theta_{10} + k_8^- \theta_9 + k_{13}^+ \theta_H + k_{11}^- \theta_*} \end{aligned}$$

Then, we obtain:

$$\theta_1 = K_1 P_1 \theta_*$$

$$\theta_H = K_2^{1/2} P_{H_2}^{1/2} \theta_{*h}$$

Surface species including **1, 2, 5, 8, 9, 10**, OH* and free θ_* sites can be described according to the steady-state approximation:

$$\theta_1 + \theta_2 + \theta_5 + \theta_8 + \theta_9 + \theta_{10} + \theta_{OH} + \theta_* = 1$$

And the other sites for H* and θ_{*h} can be described according to the steady-state approximation as summarized below:

$$\theta_H + \theta_{*h} = 1$$

$$K_2^{1/2} P_{H_2}^{1/2} \theta_{*h} + \theta_{*h} = 1$$

$$\theta_{*h} = \frac{1}{K_2^{1/2} P_{H_2}^{1/2} + 1}$$

Then, we derive an approximate expression of the formation rates for each of the major products, i.e., OL (**11**), ANE (**12**), BZ (**13**), and H₂O:

$$r_{ANE} = k_9^+ \theta_9 \theta_H$$

$$r_{OL} = k_7^+ \theta_2 \theta_H + k_{10}^+ \theta_8 \theta_H$$

$$r_{BZ} = k_{12}^+ \theta_{10} \theta_H + k_{11}^+ \theta_2 \theta_{*h}$$

$$r_{H_2O} = k_{13}^+ \theta_{OH} \theta_H$$

Thus, the relative selectivity of each product can be estimated by:

$$Selectivity_i = r_i / (r_{ANE} + r_{OL} + r_{BZ})$$

REFERENCES

1. Xiaoyang Liu, Wei An, C. Heath Turner and Daniel E. Resasco, Hydrodeoxygenation of m-cresol over bimetallic NiFe alloys: Kinetics and thermodynamics insight into reaction mechanism, *J. Catal.*, 2018, **359**, 272-286.
2. Jianmin Lu, Sina Behtash, Osman Mamun and Andreas Heyden, Theoretical Investigation of the Reaction Mechanism of the Guaiacol Hydrogenation over a Pt(111) Catalyst, *ACS Catal.*, 2015, **5**, 2423-2435.
3. Gaofeng Li, Jinyu Han, Hua Wang, Xinli Zhu and Qingfeng Ge, Role of Dissociation of Phenol in Its Selective Hydrogenation on Pt(111) and Pd(111), *ACS Catal.*, 2015, **5**, 2009-2016.
4. G. H. Gu, C. A. Mullen, A. A. Boateng and D. G. Vlachos, Mechanism of dehydration of phenols on noble metals via first-principles microkinetic modeling, *ACS Catal.*, 2016, **6**, 3047-3055.
5. A. J. R. Hensley, Y. Wang and J. S. McEwen, Phenol Deoxygenation Mechanisms on Fe(110) and Pd(111), *ACS Catal.*, 2015, **5**, 523-526.
6. <http://webbook.nist.gov/chemistry/>.